

# EXPERIMENTAL DEMONSTRATION OF WIDEBAND TUNABILITY OF AN ULTRAFAST LASER-SEEDED FREE-ELECTRON LASER

X. Yang, B. Podobedov, Y. Shen, Y. Hidaka, J. B. Murphy, and S. Seletskiy  
National Synchrotron Light Source, Brookhaven National Laboratory, Upton, NY 11973

## Abstract

We report the first experimental characterization of the wideband tunability of an ultrafast laser-seeded free-electron laser using a short seed laser pulse (140 fs in FWHM) and a variable energy electron beam. Output spectrum and pulse energy were measured versus the electron beam energy. With a 4% electron beam energy variation, an 8% spectral tuning range was observed. A significant improvement in the spectral tunability was observed using a short seed laser pulse. The experiment is in good agreement with predictions observed using the Perseo simulation code.

## INTRODUCTION

With the recent successful commissioning of the Linac Coherent Light Source (LCLS) at SLAC, free electron lasers (FELs) are widely recognized as the next-generation source of tunable, intense, coherence photons of either ultra-short time resolution or ultra-fine spectral resolution, from THz to the hard X-ray regime. Several major approaches for single-pass FELs, a Self-Amplified Spontaneous Emission (SASE) FEL [1, 2], a laser seeded FEL amplifier [3], and a spatial-bunched coherent emission FEL, such as the High Gain Harmonic Generation (HG) FELs and the Echo Enhanced Harmonic Generation (EEHG) FELs [4, 5], are currently being pursued. In the SASE configuration, the initial seed comes from the spontaneous emission of the electron beam. SASE-based devices generate tunable radiation at short wavelengths with high peak power ( $\sim$ GW), excellent transverse coherence, but rather poor temporal and spectral stability and longitudinal coherence. A way to overcome the limits of the SASE configuration is to inject the gain medium with a co-propagating phase coherent source such as a laser [5-7]. The coherence properties, both transverse and longitudinal, are preserved in the FEL output.

However, in the laser seeding configuration, the wavelength of the output FEL radiation is centered at the wavelength of the seed laser instead of at the resonant wavelength determined by the electron beam energy [8]. The tunability of the laser seeded FEL is limited by the available seed source, especially at the shorter wavelengths. Fortunately, it has been suggested recently that some tunability may be recovered by using a short broad-band seed pulse [9, 10]. Also, the advances in laser technology have made available very short and intense laser pulses which can be used to seed a high-gain single-pass FEL amplifier. With these seed pulses, a regime of the FEL interaction where the radiation evolution is simultaneously dominated by nonlinear effects

(saturation) and time-dependent effects (slippage) can be explored [11, 12].

In this paper, we report on a single-pass, laser seeded FEL amplifier experiment and simulation using a short seed laser pulse (140 fs in FWHM) and a variable energy electron beam. A wideband spectral tunability was experimentally demonstrated for the first time. The output spectrum and the radiation power were measured as the electron energy was scanned. This work demonstrates a significant spectral tuning range over 755 nm to 820 nm, about 8%. The peak FEL efficiency was doubled over the efficiency at resonance by the electron beam energy detuning 0.65%. We also confirm that the wavelength of the output FEL radiation is centered near the resonant wavelength instead of near the wavelength of the seed laser. All the measurements were compared to the simulations, using the Perseo simulation code [13], with extremely good agreements. It will have direct applications to both wideband tunability and short wavelength FEL light sources under development.

We start this work by illustrating the seed process at the short pulse mode using Perseo simulation. By analyzing the FEL output in both the time and the frequency dimensions, we provide an explanation of the mechanism responsible for FEL frequency shift with respect to both the resonant and the seed frequencies. At the early stage of the radiator, electrons interact with the seed laser. As the result of this interaction and the dispersion of the radiator, a coherent electron-density modulation, called micro-bunching, is created at the seed frequency  $\nu_s = c/\lambda_{\text{seed}}$ . When passing through the rest of the radiator, the bunched electrons produce FEL radiation through coherent emission, provided the emission frequency,  $\nu_{\text{FEL}}$ , being close to  $\nu_s$  and within the seed bandwidth  $\sigma_s$ . The frequency of the FEL emission depends on both the number of micro-bunches, determined by the length of the seed pulse and the gain curve of the radiator via an empirical equation [10]:

$$\nu_{\text{FEL}} = \nu_s - (\nu_s - \nu_r) \frac{\sigma_s^2}{\sigma_s^2 + \sigma_r^2}$$

Here,  $\nu_r$  is the FEL resonant frequency,  $\sigma_s$  is the seed bandwidth, and  $\sigma_r$  is the bandwidth of the gain medium, approximately equal to the Pierce parameter  $\rho$ . Our experiment and simulation were done in the machine condition when  $\sigma_s \gg \sigma_r$ ,  $\nu_{\text{FEL}}$  approximately equals to  $\nu_r$ .

## SIMULATION

In the simulation, we use parameters similar to the experiment described later in the paper, except a lower, 1 MW, seed power and a 50% increase in the length of the radiator allowing the seed pulse to slip through the entire

electron bunch. We often observe a double-peak time structure in the FEL output, shown as the black curve in Fig. 1(a) at the exit of the radiator. One peak (PK 1), earlier in time, corresponds to the seed laser pulse and its direct amplification in the FEL process. The other peak (PK 2), later in time, is generated by the coherent emission from those micro-bunched electrons, slipped through and left behind by the short seed pulse in the early stage of the radiator. The spectral integrations over and outside the seed bandwidth as the function of the detuning of the electron beam energy ( $\delta_e = (E - E_r)/E_r$ ) are shown as the black and red curves respectively in Fig. 1(b).

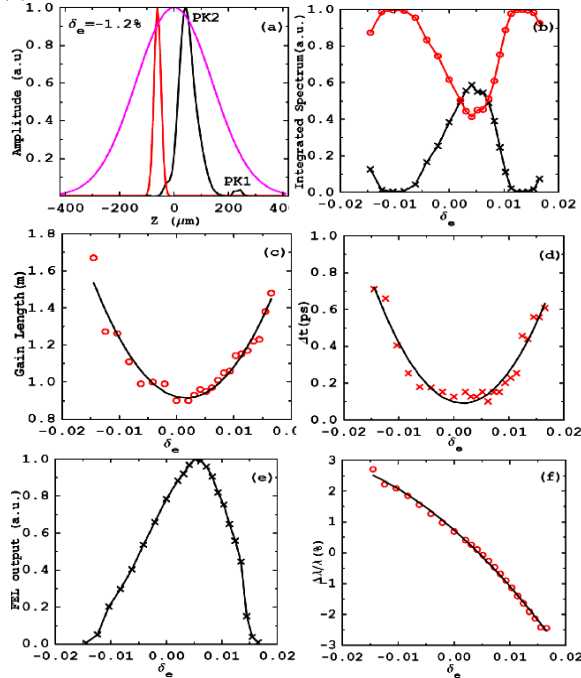


Figure 1: (a) the electron bunch (—), the seed laser pulse (—) at the entrance of the radiator, and the FEL pulse (—) at the exit of the radiator. (b) spectral integration over (—) and outside (—) the seed bandwidth, (c) FEL gain length, (d) time separation between those two FEL radiation peaks, (e) FEL power output, and (f) spectral tunability  $\Delta\lambda/\lambda = (\lambda - \lambda_{\text{seed}})/\lambda_{\text{seed}}$  as a function of the energy detuning of the electron beam,  $\delta_e$ . Here,  $\lambda$  is the amplitude-weighted average wavelength of the FEL output and the center wavelength of the seed laser respectively.

Here,  $E$  and  $E_r$  are electron beam energy and resonant energy. The separation between those peaks,  $\Delta t$ , increases with  $\delta_e$ , as shown in Fig. 1(d), following the similar trend with the relationship between the gain length and  $\delta_e$ . Both fit well using quadratic formula, as shown in Fig. 1(c). Shorter the gain length, faster the electrons being bunched by the short seed pulse, and less time delay between the coherent emission generated by the bunched electrons and the seed pulse itself. The FEL output power and output spectrum detuning are plotted as a function of  $\delta_e$  in Fig. 1(e) and Fig. 1(f).

## EXPERIMENT

After we confirmed some tunability could be recovered by using a short broad-band seed pulse in the simulation, we conducted the experiment at the Source Development Laboratory (SDL) of the National Synchrotron Light Source (NSLS), Brookhaven National Laboratory.

The NSLS SDL is a laser linac facility featuring a high-brightness electron source, a 4-magnet chicane bunch compressor, and an S-band SLAC type traveling wave linac [14]. The 100 MeV high brightness electron beam passes through the NISUS radiator [15], which is a 10-m long planar undulator consisting of 16 sections of 62.5 cm each, with a period of 3.89 cm. The seed laser, which is also the photo-cathode drive laser, is a Ti:sapphire laser based on chirped pulse amplification (CPA). The amplified laser pulse is split into two, and then goes through two independent optical grating compressors. One compressed laser pulse is frequency tripled to the UV for the photo-cathode rf gun, and the other beam is compressed down to  $\sim 140$  fs (FWHM), Fourier transform limited, for the seed pulse. Using a single laser for both electron beam generation and amplifier seed minimized the timing jitter. The seed laser has the central wavelength of 793.5 nm and the bandwidth of 7.5 nm (FWHM). The principal parameters in the experiment and as used in the simulations are summarized in Table 1.

Table 1: Experimental parameters

Energy	101.37 MeV
Bunch Charge	350 pC
Peak Current	250-350 A
Bunch Duration	1-2 psec
Energy Spread	0.1%
Normalized Emittance	4 mm-mrad
Seed Power	1-30 MW

SASE was first used to optimize the electron beam and the trajectory correction inside the radiator. To ensure the electron energy is on-resonance, the center of the SASE spectrum was set to coincide with the seed laser by adjusting the electron energy. The FEL evolution was characterized by steering the electrons to the wall using the four-wire correctors at each section to terminate the interaction at various points along the radiator.

Experimental measurements of the output FEL spectrum were taken over a range of beam energies from 99.7 to 103.8 MeV. The jitter in the electron beam energy on any given run is about 0.5% peak to peak. Time-domain simulations with Perseo have been performed to compare experiment with numerical simulations, where we use Gaussian temporal profile models cutoff at six sigma for both the electron bunch and the seed laser pulse.

The spectra of seeded FEL pulses were measured using a single-shot Ocean Optics spectrometer with a resolution of about 0.3 nm. By adjusting the electron beam energy above and below the resonant energy

$\gamma_r = \sqrt{\frac{\lambda_w}{2\lambda_r} \cdot \left(1 + \frac{k^2}{2}\right)}$ , we observed significant

changes in the FEL spectra, see Figs. 2(a) and (b). The main peak due to the electrons micro-bunched by the seed pulse in the beginning of the radiator, essentially follows  $\lambda_r$ . The experimental and simulated spectra are in substantial agreement as to the peak in the wavelength and the spectral width, except some minor details. There are more structures in the experimental spectrum compared to the simulated spectrum, and this could be explained by uncertainties in the electron energy distribution. Both experiment and simulation show that the spectrum is mainly determined by the wavelength of the resonance instead of the wavelength of the seed laser pulse.

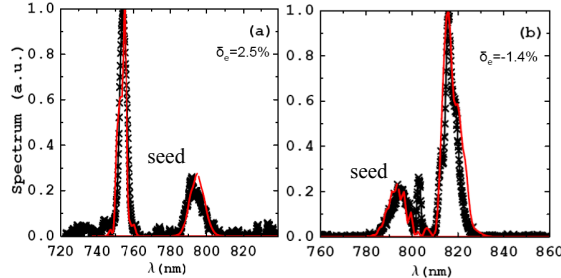


Figure 2: Comparison of spectra from experiment (—) and simulation (—) at the electron beam energy detuning (a) 2.5%, (b) -1.4%.

Experimental measurements of the output pulse energy and spectrum were taken at the -1.1% electron beam energy detuning 100.25 MeV due to the filter availability. Two band-pass filters with center frequency of 790 nm and 810 nm were inserted to measure the spectral content determined by the wavelength of the seed laser pulse and the spectral content determined by the wavelength of the resonance respectively. Since the resonant wavelength (811 nm) is outside the seed bandwidth, direct amplification of the seed laser couldn't produce a FEL output with the spectrum close to resonance. Those electrons are micro-bunched by the seed pulse in the early stage of the radiator and radiate more like a SASE with enhanced longitudinal coherence. Each filter has a 10 nm pass-band (FWHM). Without any filter, SASE output was 0.4  $\mu$ J, as shown in Fig. 3(a). The spectrum was spiky due to the lack of longitudinal coherence. The output directly amplified by the seed laser pulse was measured when the 790-nm filter was inserted, as shown in Fig. 3(b), and it was 2.5  $\mu$ J. The output from micro-bunched electrons was measured when the 810-nm filter was inserted, as shown in Fig. 3(c), and it was 47  $\mu$ J at the exit of the radiator. Compared to the SASE case, an enhancement (>100) in the FEL output was observed, and also the spectrum is much cleaner. The ratio between the output of 810 nm and the output of 790 nm is about 19 according to the experiment, and it's very close to the prediction of 20 by simulation.

A comparison between the 100-shot average in the experiment and that obtained in Perseo simulation of the pulse energy radiated by the micro-bunched electrons versus position along the undulator is shown in Fig. 3(d). The energy is measured by using a trim coil located at various points along the radiator to "kick" the beam off

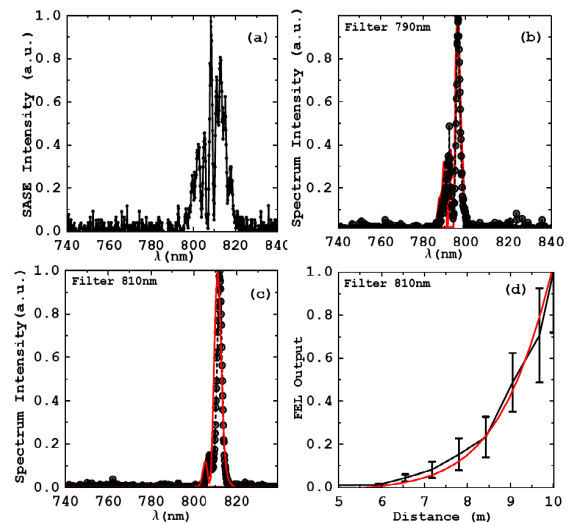


Figure 3: Comparison of spectra from experiment (—) and simulation (—) at the electron beam energy detuning -1.1% (a) SASE spectrum (—) without any filter, (b) 790 nm filter inserted, (c) 810 nm filter inserted, (d) 810 nm filter inserted, comparison of the pulse energy vs. position in experiment (—) and simulation (—).

the ideal trajectory thereby terminating the FEL interaction. The output radiation is directed to a diagnostic station where the radiation passes through the 810 nm band-pass filter and a multilayer filter to attenuate the pulse energy after which the pulse energy is measured using a calibrated joulemeter. The timing jitter between the seed laser and the electron beam, plus fluctuations in the electron beam, leads to shot-to-shot fluctuations in the FEL output reflected in the figure by the root-mean-square (rms) error bars. There a good agreement between the measurements and the simulation. The coherent radiation from the micro-bunched electron is still in the exponential gain region at the exit of the radiator.

Comparison between the experiment and Perseo simulations of the output pulse energy and the spectral peak versus the electron beam energy detuning  $\delta_e$  are shown in Figs. 4(a) and (b), where the data are represented using black dash line with rms error bars. It is evident that the output energy increases with the detuning of the beam energy from resonance. Both experiment and simulation show that the enhancement occurs when the beam energy is increased by about 0.65% from the resonant energy, while a decrease by a similar amount significantly reduces the FEL efficiency. The largest enhancement found in simulation is close to what observed in the experiment. The output spectral peak is closer to the resonant wavelength instead of the wavelength of the seed laser pulse. The output spectrum is determined by the weighted average of the two frequencies, the seed laser and the FEL resonance, according to Eq.(1) with the weighting factors proportional to the inverse of the corresponding squares of the bandwidth [10],  $\sim 10^{-4}$  and  $10^{-6}$ . We are in the limit case in which the bandwidth of the seed laser  $10^{-2}$  is significantly larger than the resonant bandwidth, which is proportional to the Pierce parameter  $\rho$ ,  $10^{-3}$ , the output

spectrum is dominated by the resonance, as shown in Fig. 4(b).

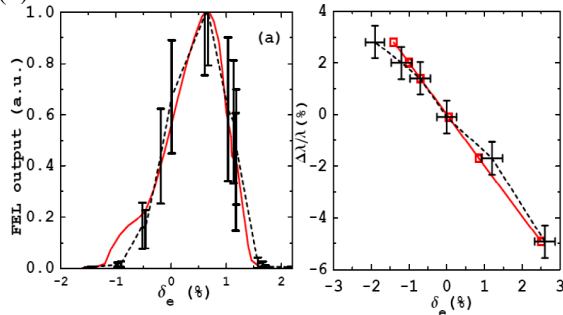


Figure 4: Comparison between experiment (---) and simulation (—) (a) the variation in output pulse energy with electron beam energy, (b) the variation of the peak spectrum detuning  $\Delta\lambda/\lambda$  with electron beam energy.

Since the spectrometer is more sensitive compared to the joulemeter, the electron beam energy detuning can be extended to a wider range in the spectral measurement, as shown in Fig. 4(b), and a significant spectral tuning range of 8% is observed. We use a factor of three in amplitude growth as the cutoff criteria defining the electron beam energy detuning range, by comparing the amplitude of the spectral peak in the seed case to that in the SASE case.

## CONCLUSION

In conclusion, we have observed the wideband tunability of an ultrafast laser seeded FEL using a short seed laser pulse (140 fs in FWHM) and a variable energy electron beam. Also, we explain such a wide spectral tunability by short seed laser pulse pre-bunching electrons via the FEL interaction and the undulator dispersion. Afterwards, those micro-bunched electrons emit coherent light at the wavelength close to that in the SASE case. However, unlike SASE, the resulting spectrum is much cleaner, and intensity is orders of magnitude higher. It will have direct applications to both wideband tunability and short wavelength FEL light sources under development.

Shorter the seed laser pulse is, larger the spectral tunability will become. A large spectral tuning range, 8%, was observed. It's significant compared with the case when the seed laser pulse is longer than the electron bunch length, the spectral tunability is negligible. The experiment is in good agreement with predictions using the Perseo simulation code.

We are grateful for support from the NSLS. This work is supported in part by U.S. Department of Energy (DOE) under contract No. DE-AC02-98CH1-886.

## REFERENCES

- [1] P. Emma for the LCLS team, "FIRST LASING OF THE LCLS X-RAY FEL AT 1.5 Å", Proc. Of PAC 2009, H3PB101 (2009).
- [2] W. Ackermann et al., Nature Photonics 1, 336 (2007).
- [3] G. Lambert et al., Nature Physics 4, 296 (2008).
- [4] G. Stupakov, Phys. Rev. Lett. 44, 5178 (2009).
- [5] Yu L. H. et al., Science, 289, 932 (2000).
- [6] R. Bonifacio et al., Nucl. Instrum. Methods Phys. Res., Sect. A 293, 627 (1990).
- [7] G. Lambert et al., Nat. Phys. 4, 296 (2008).
- [8] X.J. Wang et al., Appl. Phys. Lett. 91, 181115 (2007).
- [9] J. Wu et al., Opt. Express 16, 3255 (2008).
- [10] E. Allaria et al., EPL 89, 64005 (2010).
- [11] R. Bonifacio, et al., Phys. Rev. Lett. 73, 70 (1994).
- [12] T. Watanabe, et al., Phys. Rev. Lett. 98, 034802 (2007).
- [13] L. Giannessi, Proc. of FEL 2006, BESSY, Berlin, Germany, 91 (2006).
- [14] J. B. Murphy et al., Synchrotron Radiation News (SRN) Vol 21, No. 1, 41 (2008).
- [15] D.C. Quimby et al., Nucl. Instrum. And Method Phys. Res. Sect. A 285, 281 (1989).